RESEARCH ARTICLE
Clinical Science and Epidemiology

Whole-Genome-Sequence-Based Characterization of Extensively Drug-Resistant *Acinetobacter baumannii* Hospital Outbreak

Ghiwa Makke,[a] Ibrahim Bitar,[a,b,c] Tamara Salloum,[a] Balig Panossian,[a] Sahar Alousi,[a] Harout Arabaghian,[a] Matej Medvecky,[c,d] Jaroslav Hrabak,[b,c] Samar Merheb-Ghoussoub,[e] Sima Tokajian[a]

[a]Department of Natural Sciences, Lebanese American University, Byblos, Lebanon
[b]Department of Microbiology, Faculty of Medicine, University Hospital Pilsen, Charles University, Pilsen, Czech Republic
[c]Biomedical Center, Faculty of Medicine, Charles University, Pilsen, Czech Republic
[d]CEITEC VFU, University of Veterinary and Pharmaceutical Sciences Brno, Brno, Czech Republic
[e]Pierre and Marie Curie University, Paris, France

ABSTRACT Carbapenem-resistant *Acinetobacter baumannii* (CRAB) is an important opportunistic pathogen linked to a variety of nosocomial infections and hospital outbreaks worldwide. This study aimed at investigating and characterizing a CRAB outbreak at a large tertiary hospital in Lebanon. A total of 41 isolates were collected and analyzed using pulsed-field gel electrophoresis (PFGE). Whole-genome sequencing (WGS) was performed on all the isolates, and long-read PacBio sequencing was used to generate reference genomes. The multilocus sequence types (MLST), repertoire of resistance genes, and virulence factors were determined from the sequencing data. The plasmid content was analyzed both *in silico* and using the *A. baumannii* PCR-based replicon typing (AB-PBRT) method. Genome analysis initially revealed two clones, one carrying bla_{OXA-23} on Tn*2006* (ST-1305, ST-195, and ST-218) and another carrying bla_{OXA-72} on pMAL-1 (ST-502 and ST-2059, a new ST), with the latter having two subclones, as revealed using the Bayesian transmission network. All isolates were extensively drug resistant (XDR). WGS analysis revealed the transmission pathways and demonstrated the diversity of CRAB isolates and mobile genetic elements in this health care setting. Outbreak detection using WGS and immediate implementation of infection control measures contribute to restraining the spread and decreasing mortality.

IMPORTANCE Carbapenem-resistant *Acinetobacter baumannii* (CRAB) has been implicated in hospital outbreaks worldwide. Here, we present a whole-genome-based investigation of an extensively drug-resistant CRAB outbreak rapidly spreading and causing high incidences of mortality at numerous wards of a large tertiary hospital in Lebanon. This is the first study of its kind in the region. Two circulating clones were identified using a combination of molecular typing approaches, short- and long-read sequencing and Bayesian transmission network analysis. One clone carried bla_{OXA-23} on Tn*2006* (ST-1305, ST-195, and ST-218), and another carried bla_{OXA-72} on a pMAL-1 plasmid (ST-502 and ST-2059, a new ST). A pMAL-2 plasmid was circulating between the two clones. The approaches implemented in this study and the obtained findings facilitate the tracking of outbreak scenarios in Lebanon and the region at large.

KEYWORDS *A. baumannii*, CRAB, Tn*2006*, pMAL-1, hospital outbreak

Acinetobacter baumannii is associated with a broad range of severe wound, skin and soft-tissue, urinary tract, and bloodstream infections, secondary meningitis, and ventilator-associated pneumonia (1). These often result in extended periods of hospi-

Citation Makke G, Bitar I, Salloum T, Panossian B, Alousi S, Arabaghian H, Medvecky M, Hrabak J, Merheb-Ghoussoub S, Tokajian S. 2020. Whole-genome-sequence-based characterization of extensively drug-resistant *Acinetobacter baumannii* hospital outbreak. mSphere 5:e00934-19. https://doi.org/10.1128/mSphere.00934-19.

Editor Mariana Castanheira, JMI Laboratories

Address correspondence to Sima Tokajian, stokajian@lau.edu.lb.

Received 13 December 2019
Accepted 16 December 2019
Published 15 January 2020

talization and admission to intensive care units (ICUs) (2). *A. baumannii* survives inside human hosts, on dry surfaces, and on the hands of health care personnel for prolonged periods, and it is often associated with worldwide hospital outbreaks (3, 4).

A. baumannii infections are difficult to treat, having both intrinsic and acquired drug resistance determinants carried on plasmids, transposons, and integrons (5–7). Carbapenem resistance is mostly mediated by oxacillinases (OXAs) and less frequently by metallo-β-lactamases (MBLs) (8). The marked overproduction of class D β-lactamases (CHDLs) is the main mechanism conferring carbapenem resistance in *A. baumannii* and is caused by intrinsic genes encoding OXA-51-like enzymes and other families of OXA-type CHDLs, including OXA-23-like, OXA-40-like, OXA-58-like, and OXA-143 enzymes (9). The frequency of CHDLs and MBLs in *A. baumannii* varies in different geographic regions (10).

OXA-51 is the largest group of intrinsic OXA-type β-lactamases identified. It was originally detected in 1996 in *A. baumannii* recovered from Argentina, and later it became an important marker used for the identification of the organism at the species level (11, 12). IS*Aba1* has been identified in association with different OXA-β-lactamases, including the $bla_{\text{OXA-51-like}}$ genes. IS*Aba1* is located 7 bp upstream in the opposite direction of $bla_{\text{OXA-51-like}}$ and provides a promoter that can increase $bla_{\text{OXA-51-like}}$ gene expression levels by 50-fold (12, 13).

OXA-23 was first identified in *A. baumannii* strains isolated in the United Kingdom in 1993. Since then, it has been detected worldwide and was linked to the global dissemination of carbapenem-resistant *A. baumannii* (CRAB) (14–16). Al Atrouni et al. showed that 76.5% of the *A. baumannii* isolates collected from different hospitals in Lebanon were carbapenem resistant, with the majority (90%) harboring the OXA-23 carbapenemase (17). More recent studies revealed that carbapenem susceptibility among *Acinetobacter* isolates was 12% (18), and most of the recovered isolates (83%) were susceptible to colistin (19). Moreover, OXA-24 has several variants, including OXA-72. Isolates carrying $bla_{\text{OXA-72}}$ were associated with a number of hospital outbreaks in Spain, Ecuador, and the United States (13, 16).

In this study, we describe the molecular epidemiology of a CRAB-associated outbreak linked to Tn*2006*- and pMAL-1-mediated clones. The results obtained through whole-genome sequencing (WGS) and single-nucleotide polymorphism (SNP) analysis of 41 isolates collected in 2016 from a hospital in Lebanon were compared to the subtyping patterns obtained by pulsed-field gel electrophoresis (PFGE) and multilocus sequence typing (MLST). WGS data were additionally used to compare the two identified outbreak clones, build transmission networks, explore the genetic relatedness of the isolates causing the outbreak, study their resistomes and virulomes, and determine their circulating mobile genetic elements.

RESULTS

Clinical characteristics. A total of 41 *A. baumannii* isolates were collected between April and December 2016 from hospitalized patients. Patients' records were available for 37 of the isolates, designated ACM-1 to -37. These were recovered from 23 different patients with a mean age of 53 $\pm$ 27 years, ranging between newborn and 92 years old. Of these, 65% ($n = 15$) were females and 35% ($n = 8$) were males, and more than half of the patients (61%; $n = 14$) died due to different causes, including underlying diseases (Fig. 1; see also Table S1 in the supplemental material).

Isolates ACM-10 and -14 were found to be *A. calcoaceticus* and were not part of the outbreak. ACM-14 was used as an outgroup in the phylogenetic analysis. Isolate ACM-26 was a mixed culture (different strains of *A. baumannii*) recovered from a 3-year-old male patient.

Antibiotic susceptibility testing and resistance genes. Antibiotic susceptibility testing was performed on the 41 *A. baumannii* isolates, and 92.8% ($n = 38$) were found to be nonsusceptible to both gentamicin and amikacin. ACM-13 showed intermediate resistance to amikacin and was susceptible to gentamicin. Most of the isolates were quinolone resistant; 95% ($n = 39$) were resistant to ciprofloxacin, 92.8% ($n = 38$) were

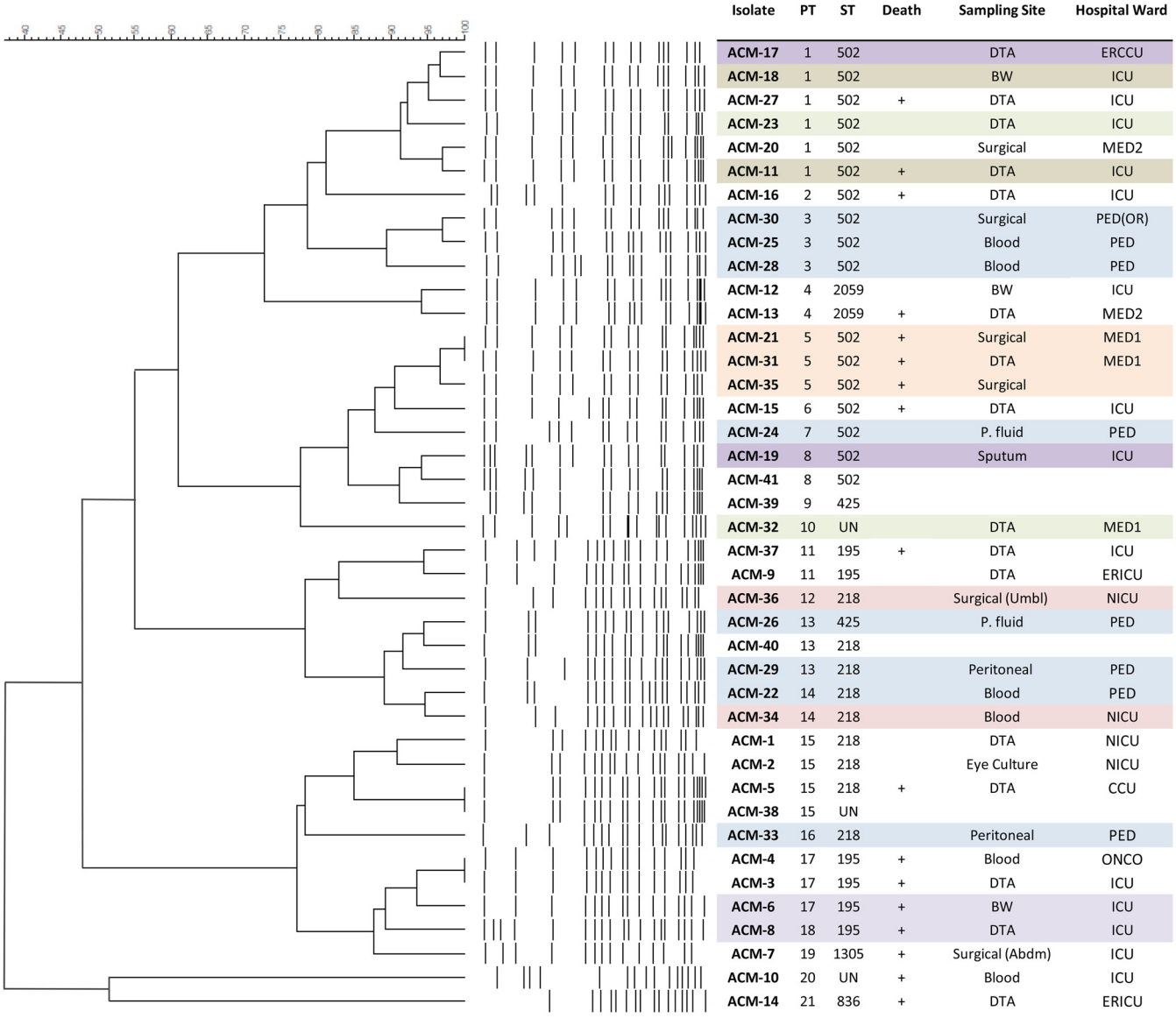

Isolate	PT	ST	Death	Sampling Site	Hospital Ward
ACM-17	1	502		DTA	ERCCU
ACM-18	1	502		BW	ICU
ACM-27	1	502	+	DTA	ICU
ACM-23	1	502		DTA	ICU
ACM-20	1	502		Surgical	MED2
ACM-11	1	502	+	DTA	ICU
ACM-16	2	502	+	DTA	ICU
ACM-30	3	502		Surgical	PED(OR)
ACM-25	3	502		Blood	PED
ACM-28	3	502		Blood	PED
ACM-12	4	2059		BW	ICU
ACM-13	4	2059	+	DTA	MED2
ACM-21	5	502	+	Surgical	MED1
ACM-31	5	502	+	DTA	MED1
ACM-35	5	502	+	Surgical	
ACM-15	6	502	+	DTA	ICU
ACM-24	7	502		P. fluid	PED
ACM-19	8	502		Sputum	ICU
ACM-41	8	502			
ACM-39	9	425			
ACM-32	10	UN		DTA	MED1
ACM-37	11	195	+	DTA	ICU
ACM-9	11	195		DTA	ERICU
ACM-36	12	218		Surgical (Umbl)	NICU
ACM-26	13	425		P. fluid	PED
ACM-40	13	218			
ACM-29	13	218		Peritoneal	PED
ACM-22	14	218		Blood	PED
ACM-34	14	218		Blood	NICU
ACM-1	15	218		DTA	NICU
ACM-2	15	218		Eye Culture	NICU
ACM-5	15	218	+	DTA	CCU
ACM-38	15	UN			
ACM-33	16	218		Peritoneal	PED
ACM-4	17	195	+	Blood	ONCO
ACM-3	17	195	+	DTA	ICU
ACM-6	17	195	+	BW	ICU
ACM-8	18	195	+	DTA	ICU
ACM-7	19	1305	+	Surgical (Abdm)	ICU
ACM-10	20	UN	+	Blood	ICU
ACM-14	21	836	+	DTA	ERICU

FIG 1 PFGE dendrogram, isolates' STs, and patients' information. PT, pulsotype; M, male; F, female; DTA, deep tracheal aspiration; P. fluid, peritoneal fluid; BW, bronchial wash; abdm, abdomen; umbl, umbilical; +, died; ICU, intensive care unit; ERICU, emergency room intensive care unit; CCU, coronary care unit; PED, pediatrics; NICU, neonatal intensive care unit; ONCO, oncology; PED(OR), pediatrics operation room; MED1, medical floor 1; MED2, medical floor 2.

resistant to levofloxacin, and one isolate (ACM-3) showed intermediate resistance to levofloxacin. Additionally, 95% ($n = 39$) were resistant to ceftazidime, imipenem, meropenem, and piperacillin-tazobactam, and 82.9% ($n = 34$) were resistant to cefepime. All isolates were susceptible to colistin, as determined by the obtained MIC values. Based on the findings described above, 95% of the isolates were classified as being extensively drug resistant (XDR) (20) (Fig. 2).

The antibiotic susceptibility testing results were confirmed through *in silico* detection of resistant determinants. Four different aminoglycoside-inactivating enzymes and their variants were detected. Aminoglycoside acetyltransferase (AAC) *aac(3′)-Ia* and *ant(3″)-Ia*, belonging to the aminoglycoside nucleotidyltransferase (ANT) family, were found in 56% ($n = 23$) and 53.6% ($n = 22$) of the isolates, respectively. Five variants of the aminoglycoside phosphotransferase (APH) enzyme were also identified. The most common was *aph(3′)-VIa*, being detected in 73% ($n = 30$) of the isolates. *strA* and *strB* variants of the *aph* enzyme were detected in 46.3% ($n = 19$), *aph(3′)-Ia* in 34% ($n = 14$), *aph(6′)-Id* in 2.4% ($n = 1$), and *armA* in 46.3% ($n = 19$) of the isolates.

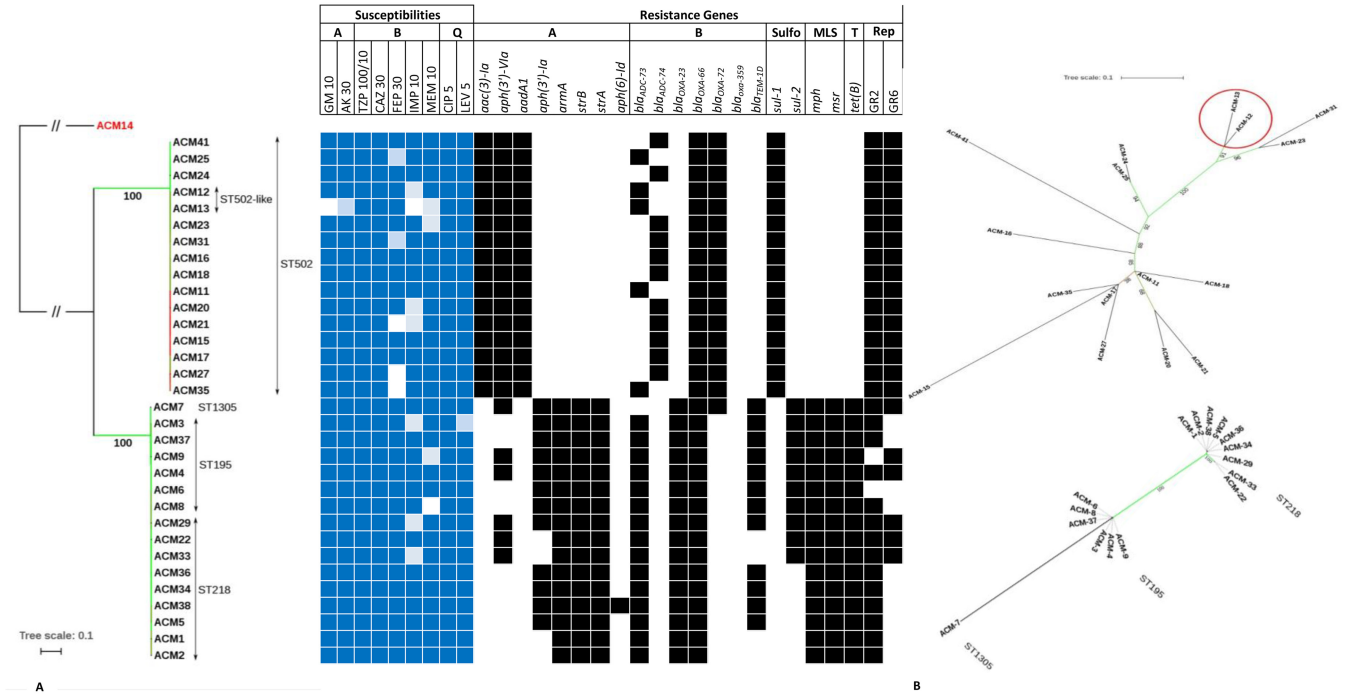

FIG 2 Maximum-likelihood phylogeny based on SNPs across *A. baumannii* isolates. (A) Branch lengths are proportional to the number of nucleotide substitutions per site. Bootstrap values are indicated by numbers below branches as well as by branch coloring (green, high confidence levels; red, low confidence levels). Dashed lines connect labels with particular leaf nodes in order to avoid labels to overlap the branches. Classes of antibiotics are given the following markings: A, aminoglycosides; B, β-lactams; Q, quinolones; T, tetracyclines; GM, gentamicin; AK, amikacin; TZP, piperacillin-tazobactam; CAZ, ceftazidime; FEP, cefepime; IMP, imipenem; MEM, meropenem; CIP, ciprofloxacin; LEV, levofloxacin. Dark blue indicates resistant, light blue indicates intermediate susceptibility, and blank indicates sensitive. (B) Unrooted phylograms inferred from SNP data from core genomes of strains belonging to the Tn*2006*-mediated clone and cluster pMAL-1-mediated clone, respectively. Red circle in the pMAL-1-mediated clone highlights ST-2059 isolates. Bootstrap values are indicated by numbers below branches as well as by branch coloring (green, high confidence levels; red, low confidence levels). Dashed lines connect labels with particular leaf nodes in order to avoid labels to overlap the branches.

Acinetobacter-derived cephalosporinase genes $bla_{\text{ADC-73}}$ and $bla_{\text{ADC-74}}$ were identified in 62.5% ($n = 25$) and 37.5% ($n = 15$) of the isolates, respectively. IS*Aba1* was detected upstream of $bla_{\text{ADC-73}}$ and $bla_{\text{ADC-74}}$ in the opposite direction. All of the isolates carried $bla_{\text{OXA-66}}$, while only ACM-14 was positive for $bla_{\text{OXA-359}}$. Class A β-lactamase ($bla_{\text{TEM-1D}}$), in addition to macrolide resistance determinants *mph*(E) and *msr*(E), were also found in 31.7% ($n = 13$) and 44% ($n = 18$) of the isolates, respectively.

PFGE. As we suspected an outbreak scenario, we first typed the isolates using PFGE. Isolates showing a difference of more than three bands were classified as belonging to different pulsotypes (21). Accordingly, 21 different pulsotypes were identified and were aligned with the STs but not with the source of isolation. The isolates, based on the PFGE output, appeared to be circulating in the different wards of the hospital. The first clade included ST-195, ST-218, ST-425, ST1305, and ST-502, while the second included ST-502 and ST-2059, a new ST, in addition to ST-218 and ST-425 (Fig. 1).

MLST. *In silico* MLST analysis, based on seven housekeeping genes (*cpn60*, *gdhB*, *gltA*, *gpi*, *gyrB*, *recA*, and *rpoD*) using the Oxford scheme, revealed the presence of eight different STs compared to only five STs identified using the Pasteur MLST scheme. Given that the Oxford MLST scheme was more capable at differentiating between closely related isolates, we adopted it for all further analysis. ST-502, CC92 (2-3-1-100-12-2-3) (ST-636, CC2 Pasteur scheme), which was the most common (44%; $n = 18$), and ST-502-like (ST-2059, a new ST), CC92 (ST-636, CC2 Pasteur scheme), were detected among the studied isolates. The difference between ST-502-like (ST-2059) and ST-502 is three point mutations in the *rpoD* gene, a G→T substitution at 117th base pair position, a G→T substitution at the 366th position, and a T→C substitution at the 504th position. ST-218, CC92 (2-3-1-102-3-2-3) (ST-2, CC2 Pasteur scheme), and ST-195, CC92 (2-3-1-96-3-2-3) (ST-2-like, CC2 Pasteur scheme), represented 27% ($n = 11$) and 17% ($n = 7$) of

the isolates, respectively. Two singletons, ST-1305, CC208 (2-3-1-96-12-2-3; ACM-7) (ST-2-like, CC2 Pasteur scheme), and ST-425, CC92 (2-3-1-100-3-2-3; ACM-39) (ST-2-like, CC2 Pasteur scheme), were also among the detected ST types.

Mobile genetic elements. The *A. baumannii* PCR-based replicon typing (AB-PBRT) method was used to characterize the circulating plasmids. AB-PBRT categorizes *A. baumannii* plasmids into homology groups (GRs) based on the nucleotide homology of their respective replicase genes. AB-PBRT results showed that 21.9% ($n = 9$) of the isolates carried homology group GR2, 2.4% ($n = 1$) carried GR6, and 68.3% ($n = 28$) carried both GR1 and GR6, related to a wide range of plasmids (22).

Tn*2006*-linked clone. Nineteen CRAB (46.3%) isolated from 14 patients carried the $bla_{\text{OXA-23}}$ carbapenemase gene in addition to intrinsically carrying $bla_{\text{OXA-66}}$. These constituted the Tn*2006*-linked circulating clone in the outbreak. $bla_{\text{OXA-23}}$ is usually associated with plasmids or integrated through transposons into the *A. baumannii* chromosome (10). These transposons are highly diverse and were designated Tn*2006*, Tn*2007*, Tn*2008*, and Tn*2009* (23). $bla_{\text{OXA-23}}$ was carried by a chromosomally integrated Tn*2006*. The mobilization of Tn*2006*, being detected in ST-195, ST-218, and ST-1305, was facilitated by the IS*Aba1* bracketing of $bla_{\text{OXA-23}}$. The remaining constituents of Tn*2006* were *yeeA* (encoding the putative DNA methylase), DEAD (encoding the putative Asp-Glu-Ala-Asp helicase), and ATPase (encoding the putative AAA ATPase) genes.

The integration site of Tn*2006* was the same among all the isolates of the Tn*2006*-linked clone. Tn*2006* was integrated inside a dienelactone hydrolase family protein, dividing it into two fragments, one 670 bp upstream of Tn*2006* and a smaller 145-bp fragment downstream of Tn*2006*.

Tn*2006* was associated with the AbaR25 resistance island, as has been previously described for Tn*2006* (23, 24). AbaR25 had the same genetic environment as AbaR25-I type (24).

The Tn*2006*-linked clone (ACM-2-6, ACM-8, ACM-9, ACM-34, ACM-36, and ACM-37) also harbored a circulating cryptic plasmid showing 100% BLAST sequence similarity to pA85-2 (GenBank accession number CP021786) and to pAB0057 (GenBank accession number CP001183) (8). The plasmid was also 99.99% similar to pAb-G7-1 (GenBank accession number KJ586856) (25), with only one base pair substitution difference (A→C). pA85-2 carried no resistance determinants but harbored a BrnT/BrnA toxin-antitoxin system, TonB-dependent receptor, and several hypothetical proteins, including septicolysin.

Interestingly, ACM-7 and ACM-28 carried both a chromosomal Tn*2006* mobilizing $bla_{\text{OXA-23}}$ and a pMAL-1 plasmid carrying $bla_{\text{OXA-72}}$, with no evidence of $bla_{\text{OXA-72}}$ exchange between the plasmid and the chromosome (Table S2).

pMAL-1-linked clone. Nineteen ST-502/2059 CRAB (48.7%) isolates were recovered from 15 patients and harbored the intrinsically carried $bla_{\text{OXA-66}}$ in addition to $bla_{\text{OXA-72}}$. Genome analysis of ACM-17, a representative of OXA-72-producing isolates, revealed that $bla_{\text{OXA-72}}$ was carried on a small 9,810-bp plasmid that was identical to a previously identified GR2 plasmid in *A. baumannii* isolated from Serbia in 2016 and designated pMAL-1 (GenBank accession no. KX230793.1). Subsequently, BLAST analysis and genome alignments showed that the remaining ST-502 isolates also carried the same pMAL-1 plasmid. This plasmid was conjugative and had a genetic backbone identical to that of pMAL-1, being in the same order and orientation as *repAci1-repAci2* (replicase genes), two XerC/XerD sites (tyrosine recombinase sites) bracketing $bla_{\text{OXA-72}}$, as well as IS*Aba31*, *tonB*, *sep* (septicolysin-encoding gene), and a few hypothetical proteins. Other plasmids were also closely related to the one detected in this study, including pA105-2 (GenBank accession number KR535993.1), isolated from *A. baumannii* in 2015, p2ABST25 (GenBank accession number AEPA01000396.1; negative for IS*Aba31*), and pAB0057 (GenBank accession number NC_011585.1; differing in the region flanking XerC/XerD; replaced by $bla_{\text{OXA-72}}$ and IS*Aba31* in pMAL-1) (Fig. 3).

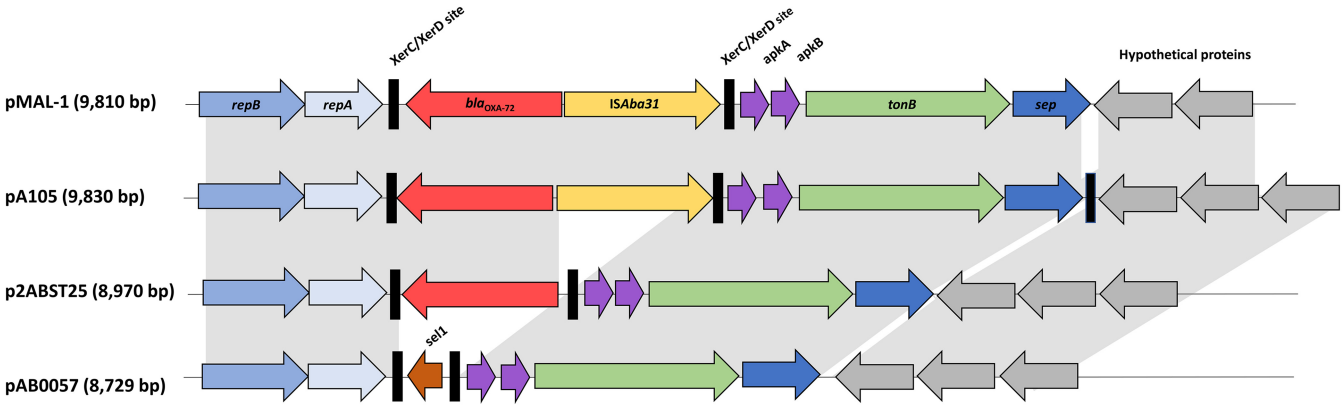

FIG 3 Comparative schematic representation of pMAL-1 and its closely related plasmids. pMAL-1 was aligned and compared with the three most closely related plasmids, pA105-2 (GenBank accession no. KR535993.1), p2ABST25 (GenBank accession no. AEPA01000396.1), and pAB0057 (GenBank accession no. NC_011585.1). Genes in pMAL-1 are annotated and colored with the following scheme: *repB*, blue; *repA*, light blue; XerC/XerD recombination sites, black; bla_{OXA-72}, red; IS*Aba31*, yellow; *apkA-apkB*, purple; *tonB*, green; *sep*, dark blue; hypothetical proteins, gray.

ACM-11, ACM-17, ACM-25, and ACM-35, which were part of the pMAL-1 clone, harbored other plasmids, such as pTG22653 (GenBank accession number CP039519.1) and ABAY04001 (GenBank accession number MK386680.1) (Table S2).

pMAL-2 circulating plasmid. In ACM-4, ACM-7, and ACM-29, representing the Tn*2006*-linked clone, and in ACM-12, ACM-15, ACM-25, ACM-31, ACM-35, and ACM-41, representing the pMAL-1-linked clone, we detected a common 70,499-bp plasmid. The plasmid was 100% identical to pAB-MAL-2 (GenBank accession number KX230794.1) (26) but had additional hypothetical proteins and a toxin-antitoxin (TA) *higAB* system. pAB-MAL-2 carried the tellurite resistance gene in addition to a Zeta toxin family protein, an ornithine cyclodeaminase, and many hypothetical proteins with unknown functions while being negative for antibiotic resistance determinants (Table S2 and Fig. S1 to S3).

In order to better characterize the *higAB* system found on pAB-MAL-2, we compared it with a recently described plasmid, pAB120, having the $higBA2_{Ab}$ TA module (27). Alignment of the TA components revealed 60.3% and 58.8% similarity to *higB2* and *higA* of pAB120, respectively. The *higAB* system was preceded by IS*Aba125* (Fig. S1). BLAST analysis showed 100% identity to *higB2* of *A. baumannii* ACICU plasmid pACICU2 (GenBank accession number CP031382) and to the type II toxin-antitoxin system RelE/ParE in many other *A. baumannii* plasmids. *higA* was 100% identical to antitoxin *higA1*, linked to *A. baumannii* ACICU plasmid pACICU2 and to transcriptional regulators in other *A. baumannii* plasmids.

Whole-genome SNP phylogenetic analysis. In total, 71,864 SNP sites were identified. Isolates were separated into two major clusters, of which two representative genomes were chosen to be additionally sequenced using PacBio long-read sequencing technology, ACM-2 (representing the isolates carrying bla_{OXA-23} and forming the Tn*2006*-mediated clone) and ACM-17 (representing the isolates carrying bla_{OXA-72} and forming the pMAL-1-mediated clones). The results obtained confirmed the presence of two circulating clones. A total of 1,207 SNP sites were detected in the Tn*2006*-linked clone, while only 57 SNPs were detected in the pMAL-1-linked clone (Fig. 2).

Outbreak analysis. To reconstruct the suspected outbreak based on statistical analyses and core genome alignments, and taking into consideration collection dates, we used the R package Outbreaker (28). Outbreaker allows for a Bayesian reconstruction of disease outbreaks by combining both epidemiologic and genomic data. As a result, a bell-shaped distribution of the mutations per site and generation was observed in the case of the Tn*2006*-linked clone, along with a tight clustering of the isolates in an interconnected nodular network (Fig. S4). Clearly localized SNP-generating hot spots were favored to produce genomic diversity, as both recombination- and non-

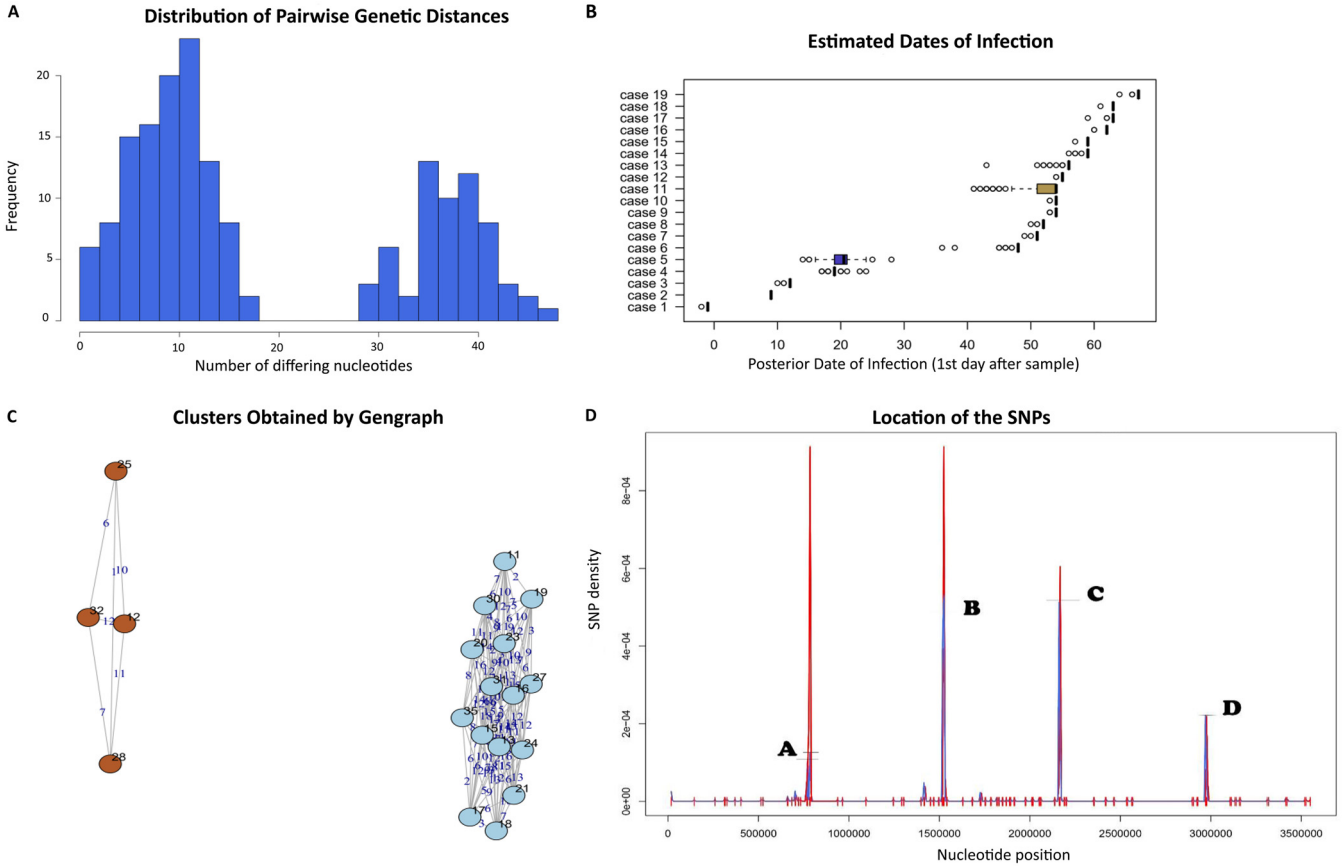

FIG 4 Bayesian transmission network analysis of the pMAL-1-mediated clone. (A) Histogram showing the distribution of pairwise genetic distances of the isolates and the relative frequencies of the genetic distances of the isolates of the pMAL-1-mediated clone. (B) Box-and-whisker plots of the estimated dates of infection. The cases are arranged based on how ancestral their core genomes are. (C) Isolates of the pMAL-1-mediated clone and their relative SNP distances from the other isolates of the cluster. At a hamming distance of 20, the isolates were arranged into two apparent subclones based on SNPs shared by some isolates in their core genomes introduced during the progression of the outbreak. (D) Graph showing the density of the SNPs relative to their positions in the genomes of the sequenced isolates: A (bp 784121), BapA prefix-like domain-containing protein; B (bp 1521949), DUF2750 domain-containing protein FDN01_10955; C (bp 2162660), stress-induced protein; D (bp 2971361), putative pilus assembly protein FilE.

recombination-induced single-nucleotide variants almost always occurred in a few defined regions (SNP density ranging from 0.0003 to 0.0012). This included genes encoding diacylglycerol kinase, 3′,5′-cyclic-nucleotide phosphodiesterase, BapA prefix-like domain-containing protein, translation error-prone DNA polymerase V autoproteolytic subunit, and epoxyqueuosine reductase QueH. An exponential decrease of the infectivity of the cases based on the probability of infecting another patient up to 20 days after infection was observed (Fig. S5).

On the other hand, in the pMAL-1-linked clone, the pairwise genetic distances had a clear bimodal distribution showing two bell-shaped curves (Fig. 4A). Based on this distribution, we speculated that the pMAL-1-linked clone encompassed two subclones. The mean mutation rate was 10, ranging from 0 to 18 for subclone I, while for subclone II we found 35 mutations, ranging between 28 and 45 (Fig. 4B). A high density of SNPs (ranging between 2×10^{-4} and 10×10^{-4}) was observed within specific loci in the core genomes. These were genes encoding BapA prefix-like domain-containing protein, DUF2750 domain-containing protein, stress-induced protein, and putative pilus assembly protein FilE.

DISCUSSION

In this study, a CRAB hospital outbreak caused by two distinct clones was tracked using PFGE, MLST, and WGS analysis over 9 months. Our analysis revealed a pMAL-1-linked clone, including ST-502 and ST-2059 isolates carrying bla_{OXA-72}, along with two

distinct subclones. A second Tn*2006*-linked clone was also identified, including ST-1305, ST-195, and ST-218 and carrying bla_{OXA-23}. Both clones were circulating in different hospital wards and causing similar rates of mortality. WGS analysis was used to understand and elucidate the transmission pathways and to demonstrate the diversity of CRAB isolates and the associated mobile genetic elements.

The mobilization and spread of the chromosomal Tn*2006* transposon to three different STs (ST-195, ST-218, and ST-1305) was facilitated by the presence of two copies of IS*Aba1* upstream and downstream of bla_{OXA-23}. Interestingly, out of the many transposons carrying the bla_{OXA-23} gene, only Tn*2006* has been shown to be highly mobile (29). bla_{OXA-23} was originally identified in *Acinetobacter radioresistens*, with bla_{OXA-23}-mediated resistance to carbapenem being detected only in the presence of a strong promoter, such as IS*Aba1* (29). IS*Aba1*, which belongs to the IS*4* family of insertion sequence elements, provides a promoter motif mediating the increased expression of bla_{OXA-23} and is involved in facilitating its own mobilization not only to *A. baumannii* but also to *Proteus mirabilis* (10). Upon its first description in 1995 in *A. baumannii*, bla_{OXA-23} carried on plasmids or transposons became widespread and was detected in isolates recovered from the United Kingdom, France, Romania, Brazil, South Korea, United Arab Emirates, Egypt, and Iraq (10, 30, 31). bla_{OXA-23} was detected previously in GC2 CRAB isolates in Lebanon and was recognized as being the most common carbapenemase in the country (17, 30). The Tn*2006*-linked clone also carried a cryptic pA85-2 plasmid that appears to be commonly found in the GC1 lineage (32). The advantage conferred by this plasmid is still unknown.

The pMAL-1-linked clone included ST-502 and ST-2059 isolates and harbored the bla_{OXA-72} gene. This is the first report of ST-502 and ST-2059 *A. baumannii* in Lebanon. Carbapenem-resistant ST-502 isolates have been reported previously in Brazil (33), Bulgaria (34), and South Africa (35). bla_{OXA-72} was first identified in 2004 in *A. baumannii* isolated from Taiwan, and since then it was detected in a few other countries, including Brazil, France, and the United States (36). The pMAL-1 plasmid was very similar to p2ABST25, with the latter being negative for IS*Aba31* (26). The presence of IS*Aba31* upstream of bla_{OXA-72} has been reported previously in pMAL-1 (26), yet its effects on bla_{OXA-72} expression require further investigations. No previous reports showed the presence of p2ABST25-positive isolates in Lebanon or any of the neighboring countries, and as such pMAL-1 could have been introduced rather than evolved from another circulating plasmid.

We also revealed that the Tn*2006*-linked clone harbored a pA85-2 plasmid carrying persistence- and virulence-related genes, such as a BrnT/BrnA toxin-antitoxin system, a TonB-dependent receptor, and a septicolysin. The BrnT toxin-antitoxin system is required for RNA cleavage and control of bacteriostasis in *Brucella abortus* (37). TonB-dependent transporters are outer membrane proteins that bind and transport siderophores in addition to vitamin B12, nickel complexes, and carbohydrates (38). Septicolysin, on the other hand, is a pore-forming toxin with cytolytic activity that mediates invasion (39).

The pAB-MAL-2 plasmid was found circulating in both the Tn*2006*- and the pMAL-1-linked outbreak clones. pAB-MAL-2 detected in this study was slightly different from that in previous reports (26). The plasmid was additionally positive for a TA system showing 60% similarity to a recently described $higBA2_{Ab}$ TA module on pAB120 (27). The *higAB* system found on the pAB-MAL-2 plasmid in our isolates was preceded by IS*Aba125*. IS*Aba125* was previously associated with the dissemination of bla_{NDM-1} (40). The presence of IS*Aba125*, a strong promoter, upstream of the TA system (41) is an important finding. TA systems are genetic loci involved in plasmid maintenance and in regulating bacterial stress responses linked to pathogen virulence and formation of drug-resistant persister cells and biofilms (42). The *higBA2* gene detected in this study is a reverse TA, where the toxin gene is the first in the operon. HigB2 functions as an RNase capable of conferring maintenance of unstable plasmid in *Acinetobacter*, and it is neutralized with HigA2 antitoxin (27).

A total of 1,207 SNP sites were detected within the Tn*2006*-linked clone harboring

bla_{OXA-23}, compared to only 57 SNP sites identified within the pMAL-1-linked clone harboring bla_{OXA-72}. Bayesian analysis revealed the transmission events with a high degree of certainty. During the outbreak, the isolates underwent genomic remodeling at clearly defined loci. Recombination events, as well as increased variance in the nucleotide sequences within a few genes, served as the primary drivers of diversity. In particular, and in both clones, a high density of SNPs was observed in BapA, a biofilm-associated protein mediating biofilm formation and adhesion to host cells (43). In the Tn*2006*-linked clone, one of the genes that accumulated a large number of SNPs encoded a diacylglycerol kinase, a small integral membrane protein (44). Diacylglycerol kinase was previously shown to be upregulated in colistin-resistant *A. baumannii* and was hypothesized to increase the integrity of the cell membrane, favoring drug resistance (45).

In conclusion, by following the pattern of transmission and based on the molecular epidemiology and genomics data, we confirm the polyclonal nature of the outbreak. Using PFGE, MLST, and PCR typing methods in combination with WGS data and SNP-based Bayesian transmission network analysis, we were able to characterize at high-scale resolution a hospital CRAB outbreak caused by a Tn*2006*-linked clone carrying bla_{OXA-23} and a pMAL-1-linked clone carrying bla_{OXA-72}. An outbreak driven by chromosomally encoded resistance determinants had a more consistent evolution and was easier to retrace using core genome sequence data from short genome reads. Alternatively, a plasmid-driven outbreak followed less of a straight evolutionary path during the sampling. Both clones additionally harbored circulating plasmids, ensuring the survival of the fittest and contributing to virulence.

MATERIALS AND METHODS

Ethical approval. Ethical approval was not required, as the isolates were collected as part of routine clinical care and patient data collection followed patient discharge from the hospital and/or death. No additional isolates were collected beyond those obtained from routine clinical care, and no diagnostic or treatment decisions were affected by the outcomes of this study.

Bacterial isolates. A total of 41 *A. baumannii* isolates were collected between April and December 2016 from hospitalized patients at a 544-bed hospital in Lebanon and were designated ACM-1 to -37 based on the date of their isolation and ACM-38 to -41 for the isolates with no trackable records. The initial identification of *Acinetobacter* species was carried out using automated microbial identification systems (Vitek and BD Phoenix).

Antimicrobial susceptibility testing. Antimicrobial susceptibility testing was performed using the disk diffusion method on Mueller-Hinton agar to determine resistance patterns against nine different antibiotics: gentamicin, amikacin, piperacillin-tazobactam, ceftazidime, cefepime, imipenem, meropenem, ciprofloxacin, and levofloxacin. The results were interpreted according to Clinical and Laboratory Standards Institute (CLSI) guidelines (M100-S29) (46). Isolates were considered extensively drug resistant (XDR) if they were nonsusceptible to at least one agent in all but two or fewer antimicrobial classes (20).

MICs were determined using the Etest (bioMérieux, France) method for gentamicin, cefepime, ciprofloxacin, trimethoprim-sulfamethoxazole, amikacin, piperacillin-tazobactam, and colistin and the broth microdilution method for colistin, meropenem, and imipenem (Sigma-Aldrich, USA). For the Etest, bacterial suspensions with turbidity equivalent to 0.5 McFarland standard were prepared and spread onto Mueller-Hinton agar (MHA) (Bio-Rad Laboratories, Inc., USA), followed by the addition of Etest strips. The plates then were incubated at 37°C for 24 h. For the broth microdilution method, cation-adjusted Mueller-Hinton broth (Sigma-Aldrich, USA) was used according to CLSI recommendations. Serial dilutions of each of the three antibiotics (32 to 0.062 μg/ml) were prepared. *A. baumannii* isolates were suspended to 0.5 McFarland turbidity and added to 96-well microdilution plates. Microplates were incubated at 35°C for 20 to 24 h. The lowest antimicrobial drug concentration at which there was no growth was considered the MIC.

PFGE. Genomic DNA plugs of *A. baumannii* were prepared according to the protocol developed by Seifert et al. (47). Briefly, plugs were digested using ApaI (Thermo Fisher Scientific, MA, USA) for 2 h at 37°C. DNA fragments were then separated on 1% Seakem Gold gel using a CHEF DR-III system (Bio-Rad Laboratories, Inc., CA, USA) for 16 h with initial and final switch time of 7 s and 20 s, respectively. To compare the patterns on different gels, *Salmonella enterica* subsp. *enterica* serovar Braenderup (ATCC BAA664TM) was used as the reference for band size using XbaI restriction digestion (Thermo Fisher Scientific, MA, USA). The gel then was stained with ethidium bromide and viewed under UV light. Fingerprints were analyzed using BioNumerics software, version 7.6.1 (Applied Maths, St-Martens-Latem, Belgium). Bands not detected automatically were manually assigned. Fingerprints were clustered according to the band-based coefficient, which measures similarity based upon common and different bands with 0.5% optimization and 0.5% tolerance of band matching.

Conjugation. Conjugation experiments were performed as described previously (48) using isolate ACM-17 of the pMAL-1-linked clone and carrying bla_{OXA-72} as a donor and *Escherichia coli* J53, resistant

to sodium azide, as a recipient. ACM-17 and *E. coli* J53 were mixed at a ratio of 4:1 (donor to recipient) in Luria-Bertani broth, and the mixture was incubated at 37°C for 1 h. To select for transconjugants, serial dilutions of the cultures were plated on UriSelect agar containing imipenem (4 μg/ml) and sodium azide (100 μg/ml).

Whole-genome sequencing. DNA extraction was performed using the NucleoSpin tissue kit (Macherey-Nagel, Germany) according to the manufacturer's instructions. Library preparation was done using the Nextera XT DNA library preparation kit (Illumina). Sequencing of the library was done on an Illumina MiSeq using a paired-end 500-cycle protocol with a read length of 250 bp. FastQC, version 1.0.0 (49), was used for quality control. Reads were trimmed by the Trimmomatic tool, v0.36 (50). Paired-end reads were assembled using SPAdes, v3.12.0 (51), and annotated using the RAST server (http://rast.nmpdr.org) (52).

Two isolates (ACM-2 and ACM-17) were additionally sequenced using PacBio long-read sequencing technology on the Sequel platform (Pacific Biosciences, CA, USA). ACM-2 represented the Tn*2006*-mediated clone, and ACM-17 represented the pMAL-1-mediated clone. Library preparation was done according to the manufacturer's instructions for microbial multiplexing. G-tubes (Covaris, USA) were used for DNA shearing, and no size selection was performed. Resulting chromosomal contigs of ACM-2 and ACM-17 were corrected by Illumina data with Pilon, v1.23 (53), and the overlapping ends of chromosomes were trimmed after manual inspection of reads mapped by BWA-MEM algorithm as implemented in BWA, v0.7.17 (54), and Bowtie, v2.3.4.2 (55). Genome assembly was done using HGAP4 (56) with minimum seed coverage of 30. PCR-based amplification was used to fill the sequence gaps.

Genome analysis. Resfinder (57), MLST 1.8 server, ISfinder database (58), BLAST (59), and the open reading frame (ORF) finder tool (59) were utilized to identify resistance genes, sequence types (STs), ISs, and plasmid identification and annotation, respectively. Mauve (version 2.3.1) was used for comparative genome alignments (60). The core genome alignments of each clone were used for outbreak analysis. Ape was used to infer basic phylogeny of the aligned core genomes (61). Adegenet was used to cluster genetic fragments that were found to be identical between the isolates from each outbreak and to perform a multivariate analysis of the genetic markers using the SeqTrack algorithm (62); this was used to visualize the genetic relatedness of the isolates spatially. plasmidSPAdes, version 3.10.1 (63), was employed to generate separate plasmid contigs, and the output was visualized through Bandage and an assembly graph viewer (64).

We used Outbreaker (28) to help elucidate the circulating clones that were directly linked to the studied outbreak. Outbreaker is based on collection dates and a reconstruction of the outbreak based on the evolution of core genome SNPs outside identified recombination spots in all studied genomes.

To detect recombinant regions, core genomes were aligned using Gubbins (65). Recombinations were masked using maskrc (https://github.com/kwongj/maskrc-svg).

Phylogenetic analysis. For the purposes of phylogenetic analysis of all the recovered isolates, along with ACM-14, which was used as an outgroup, core genome sequences were extracted from the contigs using an in-house script. The script was used to extract all nonrepetitive homologous sequences that are longer than 399 bp using NUCmer, version 3.1 (66), output as generated by QUAST, version 5.0.0 (67). Core genome sequences were aligned by MAFFT, version 7.407 (68), using default gap penalties and the memsave parameter, FFT-NS-2 strategy, and iterative refinement with a maximum of two iterations. SNP sites then were extracted from aligned sequences using the SNP-sites tool, version 2.4.0 (69).

In order to infer the phylogeny of the two clones, quality-trimmed Illumina reads were mapped to the chromosomal sequences (ACM-2 or ACM-17) using Bowtie, version 2.3.4.2 (55). SNPs were consequently called using VarScan, version 2.4.3 (70), with minimum read depth set to 8, minimum base quality of 20, and variant allele frequency of $\geq$0.8. All sites where at least one isolate had a read depth of $<$8 were removed from the final data sets.

All three data sets were analyzed by jModelTest, version 2.1.10, to determine the most appropriate models of nucleotide substitution (71). Phylogenetic analyses were performed by RAxML, version 8.2.10 (72), and robustness of the inferred topologies was assessed by 500-bootstrap replicate analyses. Topologies of the trees were visualized using iTOL, version 4.3.2 (73), and edited by Inkscape, version 0.92 (www.inkscape.org), and Gimp, version 2.10.6 (www.gimp.org).

Plasmid analysis. Sequence gaps resulting from short Illumina reads were closed using PCR and Sanger sequencing. Seven primer pairs were designed using SeqBuilder software (Lasergene, Madison, WI). For sequence analysis and annotation, the BLAST algorithm (www.ncbi.nlm.nih.gov/BLAST), the ISfinder database (www-is.biotoul.fr/), and the ORF finder tool (www.bioinformatics.org/sms/) were utilized. Comparative genome alignments were performed using Mauve, v2.3.1 (60).

Plasmid typing. The PCR-based replicon typing method for *A. baumannii* developed by Bertini et al. (22) was used to determine the plasmid content of the 41 isolates. With this method, the 27 known *A. baumannii* replicase (rep) genes are grouped into 19 homology groups according to their nucleotide sequence similarities. Six multiplex PCRs were done using primers designed by Bertini et al. (22).

Accession number(s). The draft genomes were deposited in the NCBI databases under the accession numbers listed in Table S3 in the supplemental material.

SUPPLEMENTAL MATERIAL

Supplemental material is available online only.

FIG S1, TIF file, 0.7 MB.

FIG S2, TIF file, 0.8 MB.

FIG S3, TIF file, 0.7 MB.

FIG S4, TIF file, 0.9 MB.
FIG S5, TIF file, 1.3 MB.
TABLE S1, PDF file, 0.1 MB.
TABLE S2, PDF file, 0.03 MB.
TABLE S3, PDF file, 0.02 MB.

ACKNOWLEDGMENTS

This work was partially financed by the School of Arts and Sciences Research and Development Council at the Lebanese American University and by the National Sustainability Program I (NPU I; grant number LO1503), provided by the Ministry of Education Youth and Sports of the Czech Republic, the Charles University Research Fund–PROGRES (grant number Q39), and project no. CZ.02.1.01/0.0/0.0/16_019/0000787, Fighting Infectious Diseases. The funders had no role in study design, data collection and interpretation, or the decision to submit the work for publication.

REFERENCES

1. Antunes LC, Visca P, Towner KJ. 2014. *Acinetobacter baumannii*: evolution of a global pathogen. Pathog Dis 71:292–301. https://doi.org/10.1111/2049-632X.12125.
2. Maragakis LL, Perl TM. 2008. *Acinetobacter baumannii*: epidemiology, antimicrobial resistance, and treatment options. Clin Infect Dis 46:1254–1263. https://doi.org/10.1086/529198.
3. Sunenshine RH, Wright MO, Maragakis LL, Harris AD, Song X, Hebden J, Cosgrove SE, Anderson A, Carnell J, Jernigan DB, Kleinbaum DG, Perl TM, Standiford HC, Srinivasan A. 2007. Multidrug-resistant *Acinetobacter* infection mortality rate and length of hospitalization. Emerg Infect Dis 13:97–103. https://doi.org/10.3201/eid1301.060716.
4. Kanamori H, Parobek CM, Weber DJ, van Duin D, Rutala WA, Cairns BA, Juliano JJ. 2015. Next-generation sequencing and comparative analysis of sequential outbreaks caused by multidrug-resistant *Acinetobacter baumannii* at a large academic burn center. Antimicrob Agents Chemother 60:1249–1257. https://doi.org/10.1128/AAC.02014-15.
5. Adams MD, Goglin K, Molyneaux N, Hujer KM, Lavender H, Jamison JJ, MacDonald IJ, Martin KM, Russo T, Campagnari AA, Hujer AM, Bonomo RA, Gill SR. 2008. Comparative genome sequence analysis of multidrug-resistant *Acinetobacter baumannii*. J Bacteriol 190:8053–8064. https://doi.org/10.1128/JB.00834-08.
6. Dijkshoorn L, Nemec A, Seifert H. 2007. An increasing threat in hospitals: multidrug-resistant *Acinetobacter baumannii*. Nat Rev Microbiol 5:939–951. https://doi.org/10.1038/nrmicro1789.
7. Fournier PE, Richet H. 2006. The epidemiology and control of *Acinetobacter baumannii* in health care facilities. Clin Infect Dis 42:692–699. https://doi.org/10.1086/500202.
8. Higgins PG, Dammhayn C, Hackel M, Seifert H. 2010. Global spread of carbapenem-resistant *Acinetobacter baumannii*. J Antimicrob Chemother 65:233–238. https://doi.org/10.1093/jac/dkp428.
9. Lee CR, Lee JH, Park M, Park KS, Bae IK, Kim YB, Cha CJ, Jeong BC, Lee SH. 2017. Biology of *Acinetobacter baumannii*: pathogenesis, antibiotic resistance mechanisms, and prospective treatment options. Front Cell Infect Microbiol 7:55. https://doi.org/10.3389/fcimb.2017.00055.
10. Poirel L, Nordmann P. 2006. Carbapenem resistance in *Acinetobacter baumannii*: mechanisms and epidemiology. Clin Microbiol Infect 12:826–836. https://doi.org/10.1111/j.1469-0691.2006.01456.x.
11. Brown S, Young HK, Amyes SG. 2005. Characterization of OXA-51, a novel class D carbapenemase found in genetically unrelated clinical strains of *Acinetobacter baumannii* from Argentina. Clin Microbiol Infect 11:15–23. https://doi.org/10.1111/j.1469-0691.2004.01016.x.
12. Howard A, O'Donoghue M, Feeney A, Sleator RD. 2012. *Acinetobacter baumannii*: an emerging opportunistic pathogen. Virulence 3:243–250. https://doi.org/10.4161/viru.19700.
13. Evans BA, Amyes SG. 2014. OXA β-lactamases. Clin Microbiol Rev 27:241–263. https://doi.org/10.1128/CMR.00117-13.
14. Perez F, Hujer AM, Hujer KM, Decker BK, Rather PN, Bonomo RA. 2007. Global challenge of multidrug-resistant *Acinetobacter baumannii*. Antimicrob Agents Chemother 51:3471–3484. https://doi.org/10.1128/AAC.01464-06.
15. Mugnier PD, Poirel L, Naas T, Nordmann P. 2010. Worldwide dissemination of the bla_{OXA-23} carbapenemase gene of *Acinetobacter baumannii*. Emerg Infect Dis 16:35–40. https://doi.org/10.3201/eid1601.090852.
16. Chen Y, Yang Y, Liu L, Qiu G, Han X, Tian S, Zhao J, Chen F, Grundmann H, Li H, Sun J, Han L. 2018. High prevalence and clonal dissemination of OXA-72-producing *Acinetobacter baumannii* in a Chinese hospital: a cross sectional study. BMC Infect Dis 18:491. https://doi.org/10.1186/s12879-018-3359-3.
17. Al Atrouni A, Hamze M, Jisr T, Lemarié C, Eveillard M, Joly-Guillou ML, Kempf M. 2016. Wide spread of OXA-23-producing carbapenem resistant *Acinetobacter baumannii* belonging to clonal complex II in different hospitals in Lebanon. Int J Infect Dis 52:29–36. https://doi.org/10.1016/j.ijid.2016.09.017.
18. Moghnieh R, Araj GF, Awad L, Daoud Z, Mokhbat JE, Jisr T, Abdallah D, Azar N, Irani-Hakimeh N, Balkis MM, Youssef M, Karayakoupoglou G, Hamze M, Matar M, Atoui R, Abboud E, Feghali R, Yared N, Husni R. 2019. A compilation of antimicrobial susceptibility data from a network of 13 Lebanese hospitals reflecting the national situation during 2015–2016. Antimicrob Resist Infect Control 8:41. https://doi.org/10.1186/s13756-019-0487-5.
19. Chamoun K, Farah M, Araj G, Daoud Z, Moghnieh R, Salameh P, Saade D, Mokhbat J, Abboud E, Hamze M, Abboud E, Jisr T, Haddad A, Feghali R, Azar N, El-Zaatari M, Chedid M, Haddad C, Zouain Dib Nehme M, Barakat A, Husni R, Lebanese Society of Infectious Diseases Study Group (LSID Study Group). 2016. Surveillance of antimicrobial resistance in Lebanese hospitals: retrospective nationwide compiled data. Int J Infect Dis 46:64–70. https://doi.org/10.1016/j.ijid.2016.03.010.
20. Magiorakos AP, Srinivasan A, Carey RB, Carmeli Y, Falagas ME, Giske CG, Harbarth S, Hindler JF, Kahlmeter G, Olsson-Liljequist B, Paterson DL, Rice LB, Stelling J, Struelens MJ, Vatopoulos A, Weber JT, Monnet DL. 2012. Multidrug-resistant, extensively drug-resistant and pandrug-resistant bacteria: an international expert proposal for interim standard definitions for acquired resistance. Clin Microbiol Infect 18:268–281. https://doi.org/10.1111/j.1469-0691.2011.03570.x.
21. Tenover FC, Arbeit RD, Goering RV, Mickelsen PA, Murray BE, Persing DH, Swaminathan B. 1995. Interpreting chromosomal DNA restriction patterns produced by pulsed-field gel electrophoresis: criteria for bacterial strain typing. J Clin Microbiol 33:2233–2239.
22. Bertini A, Poirel L, Mugnier PD, Villa L, Nordmann P, Carattoli A. 2010. Characterization and PCR-based replicon typing of resistance plasmids in *Acinetobacter baumannii*. Antimicrob Agents Chemother 54:4168–4177. https://doi.org/10.1128/AAC.00542-10.
23. Yoon EJ, Kim JO, Yang JW, Kim HS, Lee KJ, Jeong SH, Lee H, Lee K. 2017. The bla_{OXA-23}-associated transposons in the genome of *Acinetobacter* spp. represent an epidemiological situation of the species encountering carbapenems. J Antimicrob Chemother 72:2708–2714. https://doi.org/10.1093/jac/dkx205.
24. Kim DH, Choi JY, Kim HW, Kim SH, Chung DR, Peck KR, Thamlikitkul V, So TMK, Yasin R, Hsueh PR, Carlos CC, Hsu LY, Buntaran L, Lalitha MK, Song JH, Ko KS. 2013. Spread of carbapenem-resistant *Acinetobacter baumannii* global clone 2 in Asia and AbaR-type resistance islands. Antimicrob Agents Chemother 57:5239–5246. https://doi.org/10.1128/AAC.00633-13.
25. Hamidian M, Holt KE, Pickard D, Dougan G, Hall RM. 2014. A GC1

Acinetobacter baumannii isolate carrying AbaR3 and the aminoglycoside resistance transposon Tn*aphA6* in a conjugative plasmid. J Antimicrob Chemother 69:955–958. https://doi.org/10.1093/jac/dkt454.
26. Dortet L, Bonnin RA, Bernabeu S, Escaut L, Vittecoq D, Girlich D, Imanci D, Fortineau N, Naas T. 2016. First occurrence of OXA-72-producing *Acinetobacter baumannii* in Serbia. Antimicrob Agents Chemother 60:5724–5730. https://doi.org/10.1128/AAC.01016-16.
27. Armalytė J, Jurėnas D, Krasauskas R, Čepauskas A, Sužiedėlienė E. 2018. The *higBA* toxin-antitoxin module from the opportunistic pathogen *Acinetobacter baumannii*–regulation, activity, and evolution. Front Microbiol 9:732. https://doi.org/10.3389/fmicb.2018.00732.
28. Jombart T, Cori A, Didelot X, Cauchemez S, Fraser C, Ferguson N. 2014. Bayesian reconstruction of disease outbreaks by combining epidemiologic and genomic data. PLoS Comput Biol 10:e1003457. https://doi.org/10.1371/journal.pcbi.1003457.
29. Nigro S, Hall RM. 2015. Distribution of the bla_{OXA-23}-containing transposons Tn2006 and Tn2008 in Australian carbapenem-resistant *Acinetobacter baumannii* isolates. J Antimicrob Chemother 70:2409–2411. https://doi.org/10.1093/jac/dkv102.
30. Hammoudi D, Moubareck CA, Hakime N, Houmani M, Barakat A, Najjar Z, Suleiman M, Fayad N, Sarraf R, Sarkis DK. 2015. Spread of imipenem-resistant *Acinetobacter baumannii* co-expressing OXA-23 and GES-11 carbapenemase in Lebanon. Int J Infect Dis 36:56–61. https://doi.org/10.1016/j.ijid.2015.05.015.
31. Mugnier P, Poirel L, Pitout M, Nordmann P. 2008. Carbapenem-resistant and OXA-23-producing *Acinetobacter baumannii* isolates in the United Arab Emirates. Clin Microbiol Infect 14:879–882. https://doi.org/10.1111/j.1469-0691.2008.02056.x.
32. Hamidian M, Hawkey J, Wick R, Holt KE, Hall RM. 2019. Evolution of a clade of *Acinetobacter baumannii* global clone 1, lineage 1 via acquisition of carbapenem- and aminoglycoside-resistance genes and dispersion of *ISAba1*. Microb Genom 5:e000242. https://doi.org/10.1099/mgen.0.000242.
33. Chagas TP, Silveira MC, Albano RM, Carvalho-Assef AP, Asensi MD. 2015. Draft genome sequence of a multidrug-resistant *Acinetobacter baumannii* ST15 (CC15) isolated from Brazil. Mem Inst Oswaldo Cruz 110:691–692. https://doi.org/10.1590/0074-02760150158.
34. Pfeifer Y, Trifonova A, Pietsch M, Brunner M, Todorova I, Gergova I, Wilharm G, Werner G, Savov E. 2017. Clonal transmission of gram-negative bacteria with carbapenemases NDM-1, VIM-1, and OXA-23/72 in a Bulgarian hospital. Microb Drug Resist 23:301–307. https://doi.org/10.1089/mdr.2016.0059.
35. Lowe M, Ehlers MM, Ismail F, Peirano G, Becker PJ, Pitout JDD, Kock MM. 2018. *Acinetobacter baumannii*: epidemiological and beta-lactamase data from two tertiary academic hospitals in Tshwane, South Africa. Front Microbiol 9:1280. https://doi.org/10.3389/fmicb.2018.01280.
36. Tada T, Miyoshi-Akiyama T, Shimada K, Shimojima M, Kirikae T. 2014. Dissemination of 16S rRNA methylase ArmA-producing *Acinetobacter baumannii* and emergence of OXA-72 carbapenemase coproducers in Japan. Antimicrob Agents Chemother 58:2916–2920. https://doi.org/10.1128/AAC.01212-13.
37. Heaton BE, Herrou J, Blackwell AE, Wysocki VH, Crosson S. 2012. Molecular structure and function of the novel BrnT/BrnA toxin-antitoxin system of *Brucella abortus*. J Biol Chem 287:12098–12110. https://doi.org/10.1074/jbc.M111.332163.
38. Noinaj N, Guillier M, Barnard TJ, Buchanan SK. 2010. TonB-dependent transporters: regulation, structure, and function. Annu Rev Microbiol 64:43–60. https://doi.org/10.1146/annurev.micro.112408.134247.
39. Rosado CJ, Kondos S, Bull TE, Kuiper MJ, Law RH, Buckle AM, Voskoboinik I, Bird PI, Trapani JA, Whisstock JC, Dunstone MA. 2008. The MACPF/CDC family of pore-forming toxins. Cell Microbiol 10:1765–1774. https://doi.org/10.1111/j.1462-5822.2008.01191.x.
40. Datta S, Mitra S, Chattopadhyay P, Som T, Mukherjee S, Basu S. 2017. Spread and exchange of *bla* NDM-1 in hospitalized neonates: role of mobilizable genetic elements. Eur J Clin Microbiol Infect Dis 36:255–265. https://doi.org/10.1007/s10096-016-2794-6.
41. Lopes BS, Amyes SG. 2012. Role of IS*Aba1* and IS*Aba125* in governing the expression of bla_{ADC} in clinically relevant *Acinetobacter baumannii* strains resistant to cephalosporins. J Med Microbiol 61:1103–1108. https://doi.org/10.1099/jmm.0.044156-0.
42. Andersen SB, Ghoul M, Griffin AS, Petersen B, Johansen HK, Molin S. 2017. Diversity, prevalence, and longitudinal occurrence of type II toxin-antitoxin systems of *Pseudomonas aeruginosa* infecting cystic fibrosis lungs. Front Microbiol 8:1180. https://doi.org/10.3389/fmicb.2017.01180.
43. De Gregorio E, Del Franco M, Martinucci M, Roscetto E, Zarrilli R, Di Nocera PP. 2015. Biofilm-associated proteins: news from *Acinetobacter*. BMC Genomics 16:933. https://doi.org/10.1186/s12864-015-2136-6.
44. Smith RL, O'Toole JF, Maguire ME, Sanders CR, II. 1994. Membrane topology of *Escherichia coli* diacylglycerol kinase. J Bacteriol 176:5459–5465. https://doi.org/10.1128/jb.176.17.5459-5465.1994.
45. Park YK, Ko KS. 2015. Effect of carbonyl cyanide 3-chlorophenylhydrazone (CCCP) on killing *Acinetobacter baumannii* by colistin. J Microbiol 53:53–59. https://doi.org/10.1007/s12275-015-4498-5.
46. Clinical and Laboratory Standards Institute. 2019. Performance standards for antimicrobial susceptibility testing, 29th ed, M100. Clinical and Laboratory Standards Institute, Wayne, PA.
47. Seifert H, Dolzani L, Bressan R, van der Reijden T, van Strijen B, Stefanik D, Heersma H, Dijkshoorn L. 2005. Standardization and interlaboratory reproducibility assessment of pulsed-field gel electrophoresis-generated fingerprints of *Acinetobacter baumannii*. J Clin Microbiol 43:4328–4335. https://doi.org/10.1128/JCM.43.9.4328-4335.2005.
48. Walsh F, Cooke NM, Smith SG, Moran GP, Cooke FJ, Ivens A, Wain J, Rogers TR. 2010. Comparison of two DNA microarrays for detection of plasmid-mediated antimicrobial resistance and virulence factor genes in clinical isolates of *Enterobacteriaceae* and non-*Enterobacteriaceae*. Int J Antimicrob Agents 35:593–598. https://doi.org/10.1016/j.ijantimicag.2010.02.011.
49. Andrews S. 2010. FastQC: a quality control tool for high throughput sequence data. http://www.bioinformatics.babraham.ac.uk.
50. Bolger AM, Lohse M, Usadel B. 2014. Trimmomatic: a flexible trimmer for Illumina sequence data. Bioinformatics 30:2114–2120. https://doi.org/10.1093/bioinformatics/btu170.
51. Bankevich A, Nurk S, Antipov D, Gurevich AA, Dvorkin M, Kulikov AS, Lesin VM, Nikolenko SI, Pham S, Prjibelski AD, Pyshkin AV, Sirotkin AV, Vyahhi N, Tesler G, Alekseyev MA, Pevzner PA. 2012. SPAdes: a new genome assembly algorithm and its applications to single-cell sequencing. J Comput Biol 19:455–477. https://doi.org/10.1089/cmb.2012.0021.
52. Aziz RK, Devoid S, Disz T, Edwards RA, Henry CS, Olsen GJ, Olson R, Overbeek R, Parrello B, Pusch GD, Stevens RL, Vonstein V, Xia F. 2012. SEED servers: high performance access to the SEED genomes, annotations, and metabolic models. PLoS One 7:e48053. https://doi.org/10.1371/journal.pone.0048053.
53. Walker BJ, Abeel T, Shea T, Priest M, Abouelliel A, Sakthikumar S, Cuomo CA, Zeng Q, Wortman J, Young SK, Earl AM. 2014. Pilon: an integrated tool for comprehensive microbial variant detection and genome assembly improvement. PLoS One 9:e112963. https://doi.org/10.1371/journal.pone.0112963.
54. Li H. 2013. Aligning sequence reads, clone sequences and assembly contigs with BWA-MEM. arXiv 1303.3997 [q-bio.GN]. https://arXiv.org/abs/1303.3997.
55. Langmead B, Salzberg S. 2012. Fast gapped-read alignment with Bowtie 2. Nat Methods 9:357–359. https://doi.org/10.1038/nmeth.1923.
56. Chin C-S, Alexander DH, Marks P, Klammer AA, Drake J, Heiner C, Clum A, Copeland A, Huddleston J, Eichler EE, Turner SW, Korlach J. 2013. Nonhybrid, finished microbial genome assemblies from long-read SMRT sequencing data. Nat Methods 10:563–569. https://doi.org/10.1038/nmeth.2474.
57. Zankari E, Hasman H, Cosentino S, Vestergaard M, Rasmussen S, Lund O, Aarestrup FM, Larsen MV. 2012. Identification of acquired antimicrobial resistance genes. J Antimicrob Chemother 67:2640–2644. https://doi.org/10.1093/jac/dks261.
58. Siguier P, Perochon J, Lestrade L, Mahillon J, Chandler M. 2006. ISfinder: the reference centre for bacterial insertion sequences. Nucleic Acids Res 34:D32–D36. https://doi.org/10.1093/nar/gkj014.
59. Wheeler DL, Church DM, Federhen S, Lash AE, Madden TL, Pontius JU, Schuler GD, Schriml LM, Sequeira E, Tatusova TA, Wagner L. 2003. Database resources of the National Center for Biotechnology. Nucleic Acids Res 31:28–33. https://doi.org/10.1093/nar/gkg033.
60. Darling AC, Mau B, Blattner FR, Perna NT. 2004. Mauve: multiple alignment of conserved genomic sequence with rearrangements. Genome Res 14:1394–1403. https://doi.org/10.1101/gr.2289704.
61. Paradis E, Claude J, Strimmer K. 2004. APE: analyses of phylogenetics and evolution in R language. Bioinformatics 20:289–290. https://doi.org/10.1093/bioinformatics/btg412.
62. Jombart T. 2008. adegenet: a R package for the multivariate analysis of genetic markers. Bioinformatics 24:1403–1405. https://doi.org/10.1093/bioinformatics/btn129.
63. Antipov D, Hartwick N, Shen M, Raiko M, Lapidus A, Pevzner PA. 2016.

plasmidSPAdes: assembling plasmids from whole genome sequencing data. Bioinformatics 32:3380–3387. https://doi.org/10.1093/bioinformatics/btw493.
64. Wick RR, Schultz MB, Zobel J, Holt KE. 2015. Bandage: interactive visualization of de novo genome assemblies. Bioinformatics 31:3350–3352. https://doi.org/10.1093/bioinformatics/btv383.
65. Croucher NJ, Hanage WP, Harris SR, McGee L, van der Linden M, de Lencastre H, Sá-Leão R, Song JH, Ko KS, Beall B, Klugman KP, Parkhill J, Tomasz A, Kristinsson KG, Bentley SD. 2014. Variable recombination dynamics during the emergence, transmission and "disarming" of a multidrug-resistant pneumococcal clone. BMC Biol 12:49. https://doi.org/10.1186/1741-7007-12-49.
66. Delcher AL, Phillippy A, Carlton J, Salzberg SL. 2002. Fast algorithms for large-scale genome alignment and comparison. Nucleic Acids Res 30:2478–2483. https://doi.org/10.1093/nar/30.11.2478.
67. Gurevich A, Saveliev V, Vyahhi N, Tesler G. 2013. QUAST: quality assessment tool for genome assemblies. Bioinformatics 29:1072–1075. https://doi.org/10.1093/bioinformatics/btt086.
68. Katoh K, Standley DM. 2013. MAFFT multiple sequence alignment software version 7: improvements in performance and usability. Mol Biol Evol 30:772–780. https://doi.org/10.1093/molbev/mst010.
69. Page AJ, Taylor B, Delaney AJ, Soares J, Seemann T, Keane JA, Harris SR. 2016. SNP-sites: rapid efficient extraction of SNPs from multi-FASTA alignments. Microb Genom 2:e000056. https://doi.org/10.1099/mgen.0.000056.
70. Koboldt DC, Zhang Q, Larson DE, Shen D, McLellan MD, Lin L, Miller CA, Mardis ER, Ding L, Wilson RK. 2012. VarScan 2: somatic mutation and copy number alteration discovery in cancer by exome sequencing. Genome Res 22:568–576. https://doi.org/10.1101/gr.129684.111.
71. Darriba D, Taboada GL, Doallo R, Posada D. 2012. jModelTest 2: more models, new heuristics and parallel computing. Nat Methods 9:772. https://doi.org/10.1038/nmeth.2109.
72. Stamatakis A. 2014. RAxML version 8: a tool for phylogenetic analysis and post-analysis of large phylogenies. Bioinformatics 30:1312–1313. https://doi.org/10.1093/bioinformatics/btu033.
73. Letunic I, Bork P. 2016. Interactive tree of life (iTOL) v3: an online tool for the display and annotation of phylogenetic and other trees. Nucleic Acids Res 44:W242–W245. https://doi.org/10.1093/nar/gkw290.